

Impact of Hull Propeller Rudder Interaction on Ship Powering Assessment

Charles Badoe, University of Southampton, United Kingdom, ceb1r14@soton.ac.uk

Stephen Turnock, University of Southampton, United Kingdom, s.r.turnock@soton.ac.uk

Alexander Phillips, National Oceanography Centre, Southampton, United Kingdom, abp@noc.ac.uk

Abstract

It is the complex flow at the stern of a ship that controls the overall propulsive efficiency of the hull-propeller-rudder system. This work investigates the different analysis methodologies that can be applied for computing hull-propeller-rudder interaction. The sensitivity into which the interaction between the propeller and rudder downstream of a skeg is resolved as well as varying the length of the upstream skeg are also discussed including techniques to consider in such computations. Throughout the work, the importance of hull-propeller-rudder interaction for propulsive power enhancement is demonstrated. A final case study examines the performance of a twin skeg, twin screw arrangement.

1. Introduction

Increasing the energy efficiency of a ship will play an ever greater part in the design process. The design of the stern arrangement involving as it does the complex interaction between the hull wake, propeller performance and use of a rudder for vessel control is the dominant factor in determining the overall propulsive efficiency. The retrofit installation of energy saving devices or the improved optimisation of the stern arrangement during concept and detailed design phases require much higher fidelity analysis methods that have been conventionally applied.

The propulsive performance of a ship typically depends on how well the interaction between the hull, propeller and rudder is understood, assessed and modelled (Molland & Turnock, 2007). Sakamoto *et al.* (2013) state the relationship between the power delivered to the propeller in behind hull conditions P_D , the effective speed of a ship P_E , and quasi propulsive efficiency η_D , may be expressed as:

$$P_D = \frac{P_E}{\eta_D} = \frac{C_w + (1+k)C_f + \Delta C_f}{\frac{1-t}{1-w_T} \times \eta_R \times \left[\frac{J}{2\pi} \times \frac{K_T}{K_Q} \right]} \times \frac{1}{2} \rho S V_S^3 \quad (1)$$

where C_w is the ship wave-making resistance coefficient, k is the form factor of the ship, C_f is the frictional resistance coefficient, ΔC_f is the allowance correlation between model and ship, S is the wetted surface area of the ship, t is the thrust deduction fraction, which is the interaction between the hull and propeller, w_T is the wake fraction, which is the interaction between the hull and water, η_R is the relative rotative efficiency and takes account of the differences between the propeller in openwater condition and when behind the hull, ρ is the fluid density, J is the propeller advance coefficient, K_T is the propeller thrust coefficient, K_Q is the propeller torque coefficient.

$1-t$ and $1-w_T$ are interaction effects which play an important role in the overall powering of ships. For example, examination of equation (1) indicates how $1-t$ can be maximized and $1-w_T$ minimized to reduce the delivered power P_D . As hull-propeller-rudder interaction is dependent on many features, there is often scope for improvement in the overall ship powering process. The propeller performance will depend on the inflow (hull wake) which is also dependent on the hull form. The rudder also has to operate under the influence of the upstream hull and propeller.

This paper considers results on hull-propeller-rudder interaction and its impact on propulsive performance. The discussion is made based on the research results of a three year project on the 'Design Practice For The Stern Hull of Future Twin-Skeg Ships' at the University of Southampton, UK. The first part of the paper reviews approaches to hull-propeller rudder analyses, including various methodologies that have been used for such successful analyses, associated cost in

computation and the suitability for design purposes. The paper does not go into details of all approaches, but provides references for a more profound discussion.

The second part of the paper reviews a case study into the sensitivity into which the interaction between the propeller and rudder downstream of a skeg is resolved as well as varying the length of the upstream skeg. The computed results are compared to a detailed wind tunnel investigation, which measured changes in propeller thrust, torque and rudder forces. Variation of the upstream skeg length effectively varies the magnitude of the crossflow and wake at the propeller plane. A mesh sensitivity study quantifies the necessary number of mesh cells to adequately resolve the entire flow field. In addition, analysis is conducted on parameters such as propeller and rudder forces and rudder pressure distributions from the computation of the interaction between the skeg, rudder and propeller. The computational expense associated with the time resolved propeller interaction was identified as one of the major problems of the hydrodynamic analysis.

Lastly, based on the experience drawn from the above mentioned analysis, techniques to consider for hull-propeller-rudder applications such as a twin skeg, twin screw vessel are discussed, this includes the influence of small details that are easily not included in such computations, but can result in changes in flow characteristics as well as changes in propulsive power.

2. Approaches and methodologies

Flow analysis of a ship stern to gain an understanding of the interaction between the hull, propeller and rudder for performance improvement is a challenging task from a numerical point of view. The most interesting and challenging aspect of such analysis is the influence of the propeller action and the unsteady hydrodynamics of the rudder working in the propeller wake. One approach to address the problem is to adopt a direct method where the propeller and farfield domains are joined using a rotor-stator method (*Lübke, 2005*). The propeller is rotated at each time step and the interface between the two domains is achieved using a sliding mesh interface. To ensure the flow structure generated around the propeller are correctly transferred to the stationary domain, a fine mesh is required at the interface. This approach theoretically offers the highest degree of fidelity, but requires small time steps due to restrictions imposed by explicitly solving the propeller flow, thus placing a high demand on computation.

The next level of complexity involves using an indirect approach by coupling a lower fidelity propeller code (potential flow code, blade element momentum BEMt code etc.) with a CFD solver. The propeller code utilises the non-uniform inflow at the propeller plane calculated from the RANS simulation to determine the thrust and torque as well as its distribution. This is then represented in the RANS simulation by momentum source terms. Such an approach alleviates some of the time step and mesh restrictions. This has been used by *Simonsen and Stern (2003)* to simulate the manoeuvring characteristic of the Esso Osaka with a rudder. In their formulation the propeller was represented by bound vortex sheets placed at the propeller plane and free vortices shed downstream of it. BEMt was used by *Phillips et al. (2009)* amongst others to evaluate the momentum terms.

The lowest level of complexity involves the use of a prescribed body force approach where the impact of the propeller on the fluid is represented as a series of axial and tangential momentum sources. This is the simplest of the discussed methods, although more simplified first order methods also exist. For instance the approach with a uniform thrust distribution that has been used by *Phillips et al. (2010)* and which assumes a force only in the axial direction.

Badoe et al. (2014) investigated the three-way interaction between the hull, propeller and rudder by replicating experiments performed by FORCE Technology for a container ship operating at a Froude number of 0.202. The ability of three different methods were compared, namely; prescribed body force approach (RANS-HO), Two-way coupled RANS-BEMt model (RANS-BEMt) and a discretised propeller approach or direct method (AMI). This was validated against experimental data from the SIMMAN 2014 workshop on verification and validation of ship manoeuvring simulation methods,

SIMMAN (2014). Differences between the various methods were outlined quantitatively. The results demonstrated that as long as the radial variation in both axial and tangential momentum generated by the propeller are included in the computations, then the influence of the unsteady propeller flow can be ignored and a steady computation performed to evaluate the propeller influence on the hull and rudder. Below are other conclusions drawn from the study regarding the various methods:

(a) Fluid dynamic fidelity

RANS-HO assumes a constant circumferential distribution of thrust and torque, hence do not capture all aspects of hull-propeller-rudder interaction effects, especially the interaction between the hull on propeller and rudder on propeller and vice versa. The method was also poor in replicating the swirl effect which resulted in a different flow field (i.e. symmetry in the flow field).

RANS-BEMt is best suited for capturing and predicting most aspects of hull-propeller-rudder interaction effects. The method calculates the thrust and torque as part of the simulation and is able to replicate the swirl effect much better than RANS-HO.

AMI theoretically offers the highest degree of fidelity, however, it requires small time steps due to restrictions imposed by explicitly solving the propeller flow.

(b) Computational cost

RANS-HO is the least costly, can be used for quick resistance and self-propulsion estimations only if the flow field details are not of prime importance.

RANS-BEMt follows on from RANS-HO as being less costly for ship resistance and propulsion simulations with less than 0.27% of the total simulation (of 6 wall clock hours) spent on propeller modelling.

AMI is the most computationally demanding approach (typically $\geq 30\%$ of the total simulation time for similar setup with RANS-BEMt) since the full transient flow field needs to be resolved with a higher level of mesh cells in order to provide accurate estimates of resistance and propulsion parameters. The method does not only suffer from long overall simulation time, but also from increased computational time per time step.

(c) Suitability for design purposes

RANS-HO reasonably predicted the global forces compared to the experiment, but was poor in replicating the flow field as such the method may be used for initial assessment of ships resistance and propulsion where requirement for exact mirroring of the flow fields are not essential.

RANS-BEMt was able to predict the resistance and propulsion parameters much better, but the propeller influence has been averaged over one blade passage which neglects tip and hub vortices, this makes it unsuitable for cavitation analysis. The methods may, however benefit from the addition of tangential inflow conditions and coupled with the non-uniform inflow inputs may be suitable for transient manoeuvring simulations as well as resistance and powering computations.

AMI is more suitable for all the analysis described above, but requires experience in the use and distribution of high mesh cells to capture detail flow features.

3 Case studies

3.1. Skeg-rudder-propeller interaction review

As an example, a skeg-propeller-rudder interaction investigations in straight ahead condition and drift angle is presented (see *Badoe et al. 2015a* for full details of the study). An open source flow solver was used to investigate the sensitivity into which the interaction between the propeller and rudder downstream of a skeg is resolved as well as varying the length of the upstream skeg. In simulating the skeg, rudder and propeller flow, the entire flow field was considered as a result of the oblique motion and rotation induced by the propeller. A discretised propeller approach which uses the arbitrary mesh interface technique (AMI) was used to account for the action of the rotating propeller. Due to the complexity of the propeller geometry, especially around the blade tip with very small thickness, it was possible to place only two prism layers on the propeller. The surface refinement for the propeller was however increased to ensure that most of the flow features were resolved. Fig. 1 shows the different meshes generated on the propeller. Tables 1&2 show the details of the grid system along with predicted thrust and torque computed on each grid as well as viscous and pressure contributions to the total drag. Rudder lift and drag values are also presented for *Simonsen (2000)* and *Phillips et al. (2010)* who both performed similar investigations for straight ahead conditions (no applied angle of drift) using the CFDHIP-IOWA and ANSYS CFX code respectively, and using a body force propeller model with load distribution based on the *Hough and Ordway(HO) (1965)* thrust and torque distribution.

The difficulty associated with rudder drag prediction is evident in the results. This is mainly due to the difficulty associated with replicating the influence of swirl on the local incidence angle. At high thrust loadings, swirl components increases, leading to a reduction in the drag experienced by the rudder, the mechanism is illustrated in Fig. 2. *Simonsen (2000)* outlined other reasons for drag coefficient over prediction. Since the x-component of the normal to the rudder surface is large at the leading edge, the pressure contribution is dominant for the local drag coefficient in this region, therefore if the leading edge pressure and suction peaks are not adequately resolved it could lead to discrepancies in drag coefficient. Although the detail local flow features such as the tip and hub vortices (which are useful for cavitation analysis) described above will not be captured by the level of grid used, for manoeuvring performance of the rudder exact “mirroring” of the flow field is not essential as long as the required condition of flow (head) are adequately captured. *Phillips et al. (2009)* highlights the difficulties in the prediction of propeller torque and rudder forces with large uncertainties and comparison errors between calculated and experimental result unless significantly larger meshes are used. *Wang and Walters (2012)* indicated values in excess of 22M to resolve propeller forces, whilst *Date and Turnock (2002)* indicates values of 5-20M cells to fully resolve the rudder forces. However, a good level of understanding of the global forces required for rudder and propeller forces during manoeuvring may be obtained with the level of mesh resolution. Wall effects also play a defining role in rudder drag prediction as has been addressed by *Höerner (1965)* who showed that due to root vortex the drag of wall mounted experimental rudder differs from that of numerical rudder. Because the propeller was working close to the wind tunnel floor, it could have influenced the root flow, hence the root vortex and rudder drag prediction. Figs. 3&4 show the rudder forces for rudder angle $\alpha = -10.4^\circ$, -0.4° , and 9.6° . The results show improvement in the fine grid, especially for the drag coefficient.

3.1.1. Influence of propeller on rudder in straight ahead condition and at drift

The global forces for the rudder and propeller combination in isolation at straight ahead and drift angle conditions is shown in Fig. 5. Results for the straight ahead condition demonstrates that the wake field generated by the propeller compares well with experimental values of lift and drag on a rudder placed aft of the propeller at different angles of incidence. The influence of drift angle is well captured in terms of rudder lift and drag characteristics.

Table 1: Grid system used for sensitivity analysis.

Parameter	Coarse grid	Medium grid	Fine grid
BlockMesh refinement	80×18×36	113×24×51	160×36×72
Cells in rotating region	150K	300K	770K
Cells in stationary region	1.2M	2.9M	8.0M
Total no of cells (approx.)	1.4M	3.3M	8.8M
Computational expense	20-22hrs	60-65hrs	170-180hrs

NB: Computational expenses are based on parallel run of 12 partitions run on 6 core nodes for approximately 20 propeller revolutions. All times are in wall clock hours

The effect of the applied drift angle on the rudder results in a downward shift of the lift curve and does not significantly change the lift curve slope. Although not shown here, the applied drift angle resulted in an over prediction of propeller torque, since rudder forces are dependent on the inflow conditions (propeller race) which in turn are dominated by the action of the propeller, slight over-prediction in propeller force will result in an increased inflow velocity to the rudder, causing an increase in rudder force, hence the upward shift in rudder lift curve observed for the -7.5deg drift angle as compared with experiment. At $\alpha = -10^\circ$ (α_E of -23°), the predicted accuracy for rudder drag deteriorates. The reason is most likely that the rudder has stalled and the mesh count (of 3.3M) used to mirror entire flow field makes it difficult to capture the stall effect. The grid used, however is able to predict accurately the effective angle of attack (α_E) up to 18° ($\alpha = -5^\circ$). Fig 6 presents the axial velocity contours at three positions along the rudder at midchord, trailing edge and in the wake for the drift angle condition. It is interesting to note how the accelerated flow impinges on the rudder and the development of the tip vortices.

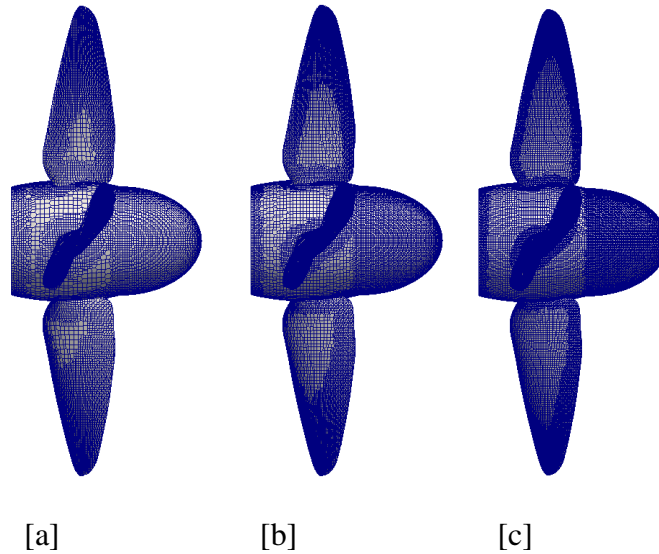


Fig.1: Mesh cut for propeller [a] coarse grid 1.4M cells [b] medium grid 3.3M cells and [c] fine grid 8.8M cells

3.1.2. Influence of skeg length on rudder-propeller performance

An upstream skeg at an angle of drift slows down the inflow to the propeller. For a rudder downstream of the propeller at drift, accurate determination of the rudder forces is influenced by the axial and tangential wake flow (Fig. 7). It can be in Fig. 8 seen that the presence of the skegs tends to reduce the lift curve slope as a result of flow straightening and there is a downward shift in the lift curve compared to the rudder and propeller alone at drift in Fig. 5. The lift curve slope, $\partial C_L / \partial \alpha$ (see Table 3) are also well predicted. The calculated drag when approaching stall was not accurately predicted due to similar reasons outlined earlier. The rudder drag at zero incidence C_{D_0} is highest for the rudder-propeller in isolation. Comparison of the plots to that of the straight ahead con-

dition in Fig 4 shows that the asymmetry in the flow results in a shift in the performance of the rudder which increases with increasing upstream skeg length. This shift may depend on the angle of drift.

Table 2: Detailed grid analysis for propeller and rudder forces, $\alpha = 10^\circ$, $\beta_R = 0^\circ$, $J = 0.36$.

Grid	Coarse grid	Medium grid	Fine grid	Simonsen (2000)	Phillips (2010)	Data
K_T	0.305	0.294	0.286			0.283
ϵ	+7.77%	+3.89%	+1.06%			
K_Q	0.051	0.047	0.044			0.043
ϵ	+18.60%	+9.30%	+2.32%			
C_L	1.350	1.280	1.220	1.270	1.360	1.251
ϵ	+7.96%	+2.36%	-2.44%	+1.56%	+8.76%	
$C_{D \text{ total}}$	0.190	0.170	0.148	0.070	0.187	0.109
ϵ	+74.3%	+55.96%	+35.78%	-93.58%	71.56	
$C_{D \text{ viscous}}$	0.075	0.072	0.069			
$C_{D \text{ pressure}}$	0.115	0.098	0.079			

At $x = 1.05$ chords, the propeller swirl dominates the flow, the rudder wake has mixed with the surrounding faster moving fluid. The overall results provide reasonable initial estimates for rudder forces at drift angle $\beta_R = -7.5^\circ$ and 0° . Overall improvements in mesh resolution around the propeller, rudder and rudder tip vortices would improve the quality of the results.

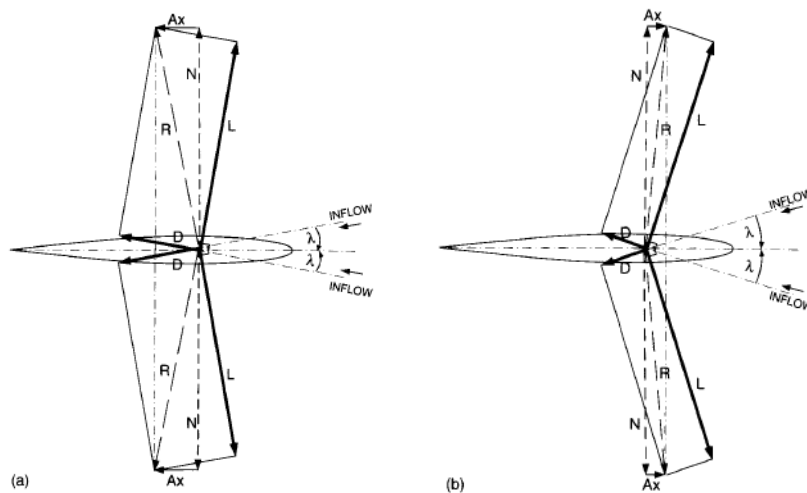


Fig.2: [a] Rudder angle zero degrees: forces due to propeller-induced incidence [b] Rudder angle zero: forces due to propeller-induced incidence - high thrust loading, source: *Molland and Turnock (2007)*.

3.1.3. Rudder pressure distribution at straight ahead and at drift conditions

The influence of the propeller and skeg on rudder at straight ahead and drift conditions are compared through chordwise pressure distribution of surface pressures for eight spanwise rudder locations from the root to tip in Fig. 9. The computed chordwise pressure distribution represented by the local pressure coefficient C_p is given by:

$$C_p = \frac{P - P_\infty}{0.5\rho U^2} \quad (2)$$

where $P - P_\infty$ is the local pressure; ρ is the density of air and U is the free stream velocity. Drift angle influence can be observed for most areas of the rudder span below the center of the slipstream (below the hub). Close to the slipstream, (span 230 & 390mm) local incidence resulted in the pressure peak increasing with increasing skeg lengths at the rudder leading edge. An area of interest was just around

the hub where the unsteadiness in the flow introduced by the hub vortex can be observed for span 530mm as a bulge in the pressure curve for the zero drift angle around the rudder trailing edge. This was not observed for the drift cases. In areas close to the tip (span 705mm-970mm) there were little or no differences in pressure curves for the drift cases. This is also seen in the streamlines passing through the short skeg at drift, Fig. 7 where most of the flow changes occur in the rudder mid span, explaining why there was little difference in pressure curves for the drift cases around the rudder tip.

Table 3: Rudder lift curve slope, $\partial C_L/\partial \alpha$, and corresponding drag at zero incidence, C_{D0} .

	C_{D0}		$\partial C_L/\partial \alpha$	
	Molland&Turnock	Calculations	Molland&Turnock	Calculations
Zero drift angle	0.016	0.02	0.132	0.129
Rudder&propeller alone	0.083	0.06	0.146	0.144
Short length skeg	0.029	0.01	0.121	0.119
Medium length skeg	0.025	0.012	0.119	0.115
Long length skeg	0.0169	0.019	0.125	0.126

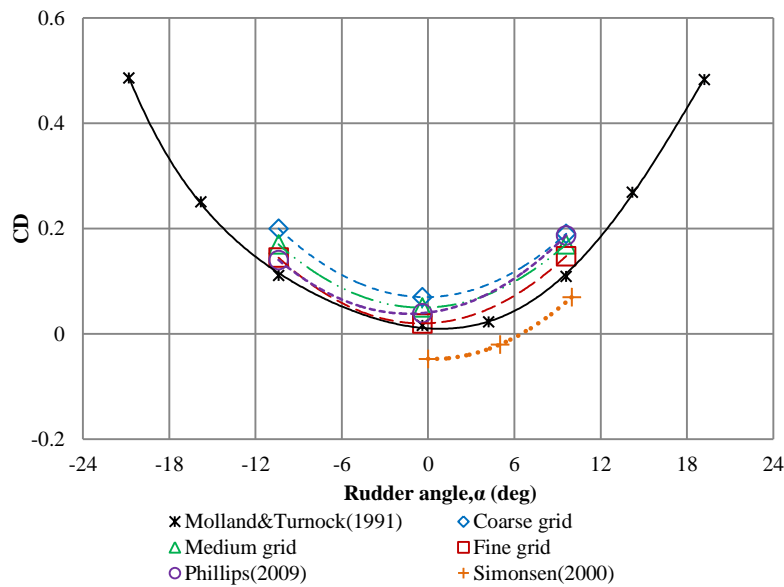


Fig.3: Rudder drag coefficient, $\beta_R = 0^0$, $J = 0.36$.

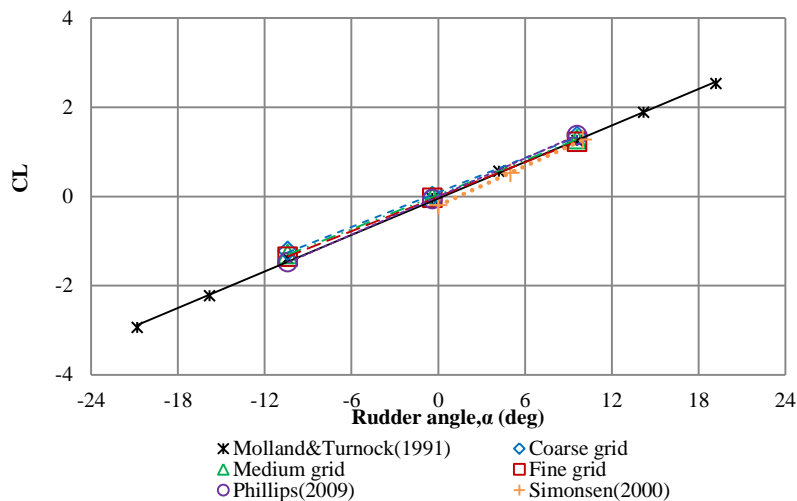


Fig.4: Rudder lift coefficient, $\beta_R = 0^0$, $J = 0.36$.

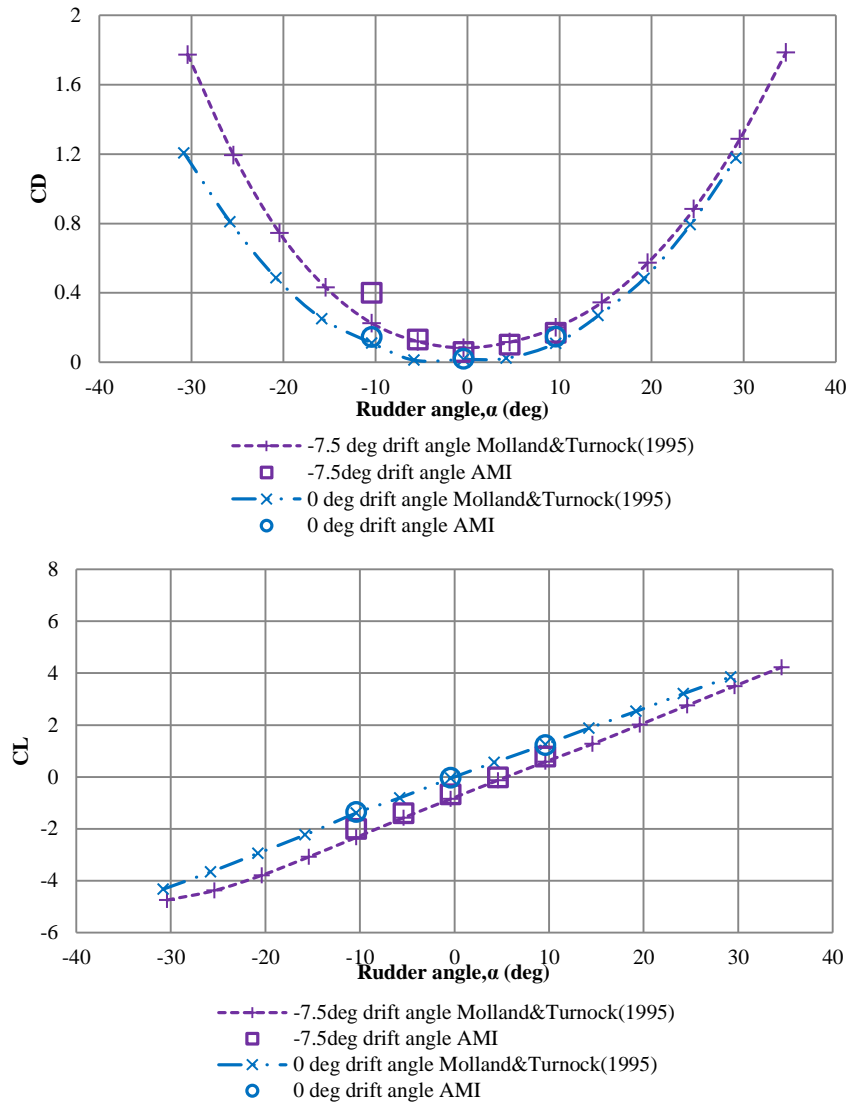


Fig.5: Effect of drift angle on the performance of a rudder and propeller combination in isolation at $J = 0.36$, $\beta_R = -7.5^\circ$ (medium grid results) and $\beta_R = 0^\circ$ (fine grid results).

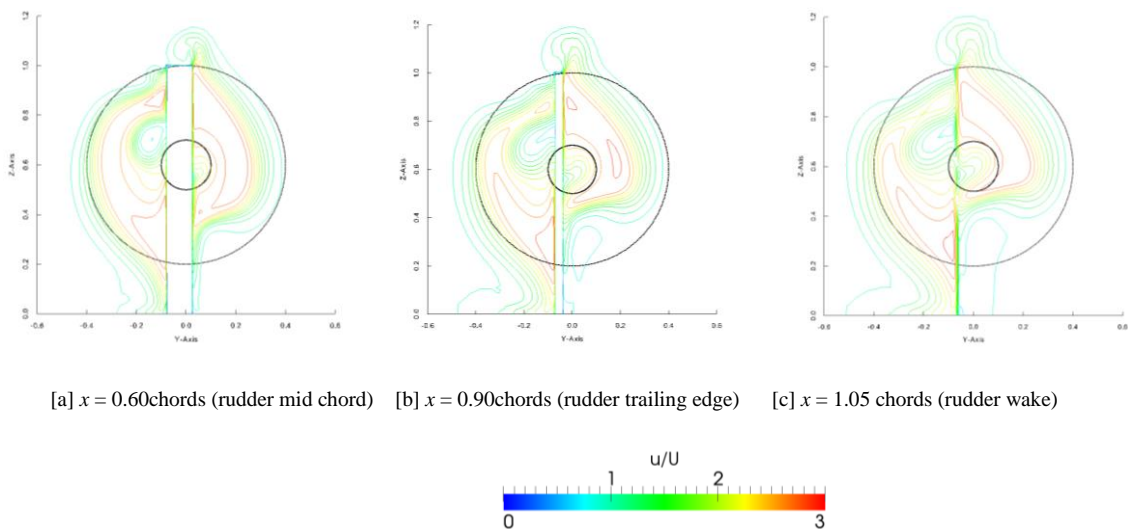


Fig.6: Axial velocity contours at different rudder x -positions, $J = 0.36$, $\beta_R = -7.5^\circ$ at $\alpha = 10^\circ$.

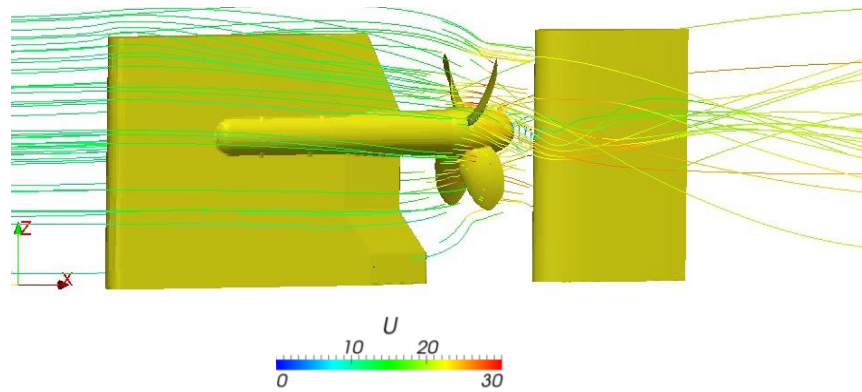


Fig.7: Streamlines passing through the shortskeg, $J = 0.36$, $\beta_R = -7.5^\circ$ at $\alpha = 10^\circ$.

3.2. Techniques to consider for effective hull-propeller-rudder computations

Various techniques to consider in ship powering based computations, including small details that can result in changes in flow characteristics as well as changes in propulsive power:

- High fidelity computations

Using Reynolds Averaged Navier Stokes solvers (RANS) to analyse hull-propeller-rudder require high fidelity computations as the boundary layer of the hull, skeg and the viscous wake needs to be captured with high level of accuracy. Here, high fidelity refers to RANS solvers which employ good grids and strong turbulence models. The skeg and hull flow may be characterised by complex vortex shedding, which may require complex grid resolution in order to understand them. *Eça et al. (2002)* showed that numerical simulation of such flows require grids with orthogonality at the ship surface where the no-slip condition is applied and high stretching of the grid towards that surface to resolve the flow in the near-wall region. The mesh in the propeller plane should be able to give circumferential distribution of the three components of the velocity as this information forms an important part of the input to the propeller. It is not always the size of the grid that determines the accuracy of the solution but its distribution so as to provide useful information of the underlying physics of the flow.

- What if the self-propelled thrust is over estimated ?

Reference is hereby made to *Badoe et al. 2015b* who focussed on calm water powering performance of a future twin skeg LNG ship specifically on the changes in propulsive power resulting from small variations in design. The influence of free surface was not included in the computations. A 'RANS-BEMt' approach was utilized for the self-propelled computations. The self-propulsion point was realised by manually adjusting the propeller revolutions until the self-propelled thrust (T_{sp}) equals the self-propelled drag (R_{sp}) or $T_{sp} - R_{sp} = 0$, similar to actual model test procedures. Fig. 10 shows the impact on thrust deduction when the self-propelled thrust is over-estimated. From the plot, it can be seen that a linear relation exists between self-propelled thrust prediction and its impact on thrust deduction. For example, from the results, an error of the self-propelled thrust by say 7% will result in an error in the thrust deduction by approximately 7%. It should however be pointed out that this relation has been found based on constraints placed on the hull and the use of nominal wake values as input to the propeller code.

- Tangential wake effects

A disadvantage with the equipment of skegs is that they have a high wetted surface area, hence increasing frictional resistance. But as may be seen from the streamline plot in Fig. 11, the presence of the skegs provides pre swirl to the propeller. This is advantageous for the

propeller performance as it can contribute to improving the propeller efficiency, compensating for increase in frictional resistance. Most self-propelled twin skeg computations using a body force propeller model only consider the effect of axial wake as that is the predominant component as far as most propeller straight ahead flows are concerned. Usually, an upward flow exists at the aft end which leads to an axial flow component plus a tangential flow component (Molland et al. 2011). The influence of tangential wake was studied by Badoe et al. 2015b for a twin skeg ship as shown in Fig. 12. The plots were taken at 0.18D behind the propeller plane (see Fig.13). The influence of tangential wake investigated showed that by considering the upward flow the true axial component is slightly over-predicted, both the radial and tangential components of wake are modified thus modifying the thrust deduction and hence the propulsive efficiency.

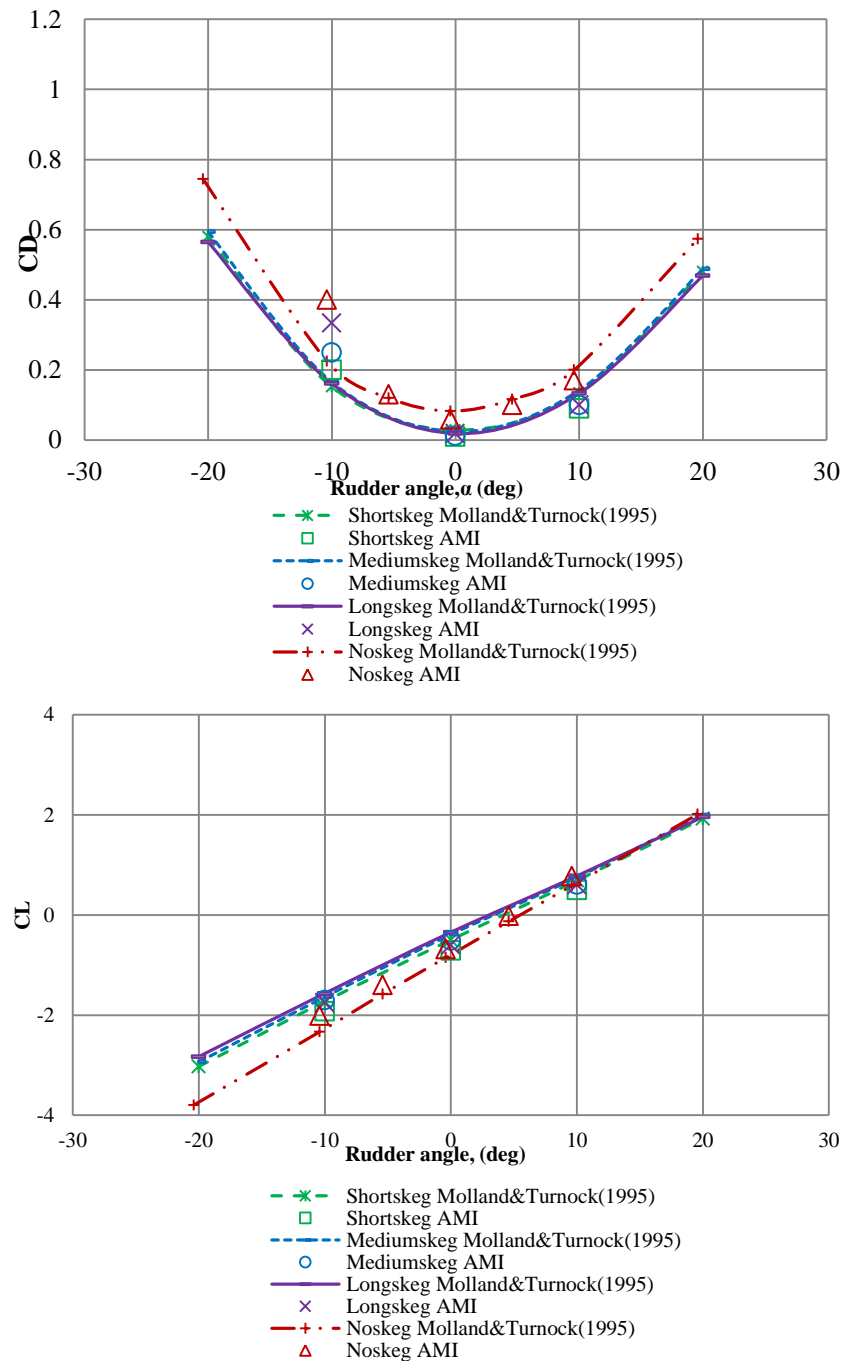


Fig. 8: Effect of drift angle rudder downstream of 3 skeg configurations at $J = 0.36$, $\beta_R = -7.5^\circ$

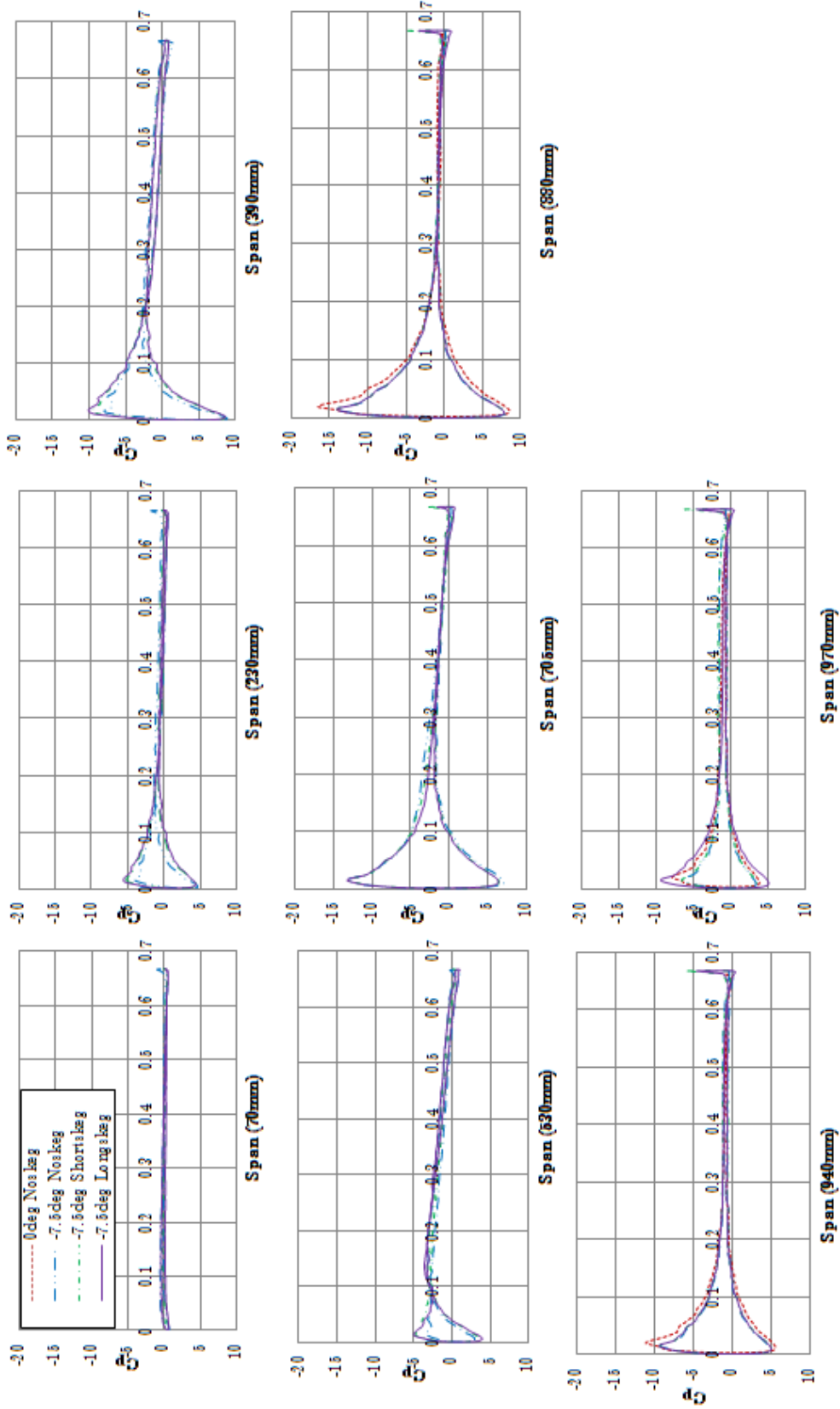


Fig. 9: Chordwise pressure distribution at various rudder spanwise positions, $J = 036$, $\beta_R = -7.5^\circ$ & 0° , $\alpha = 10^\circ$.

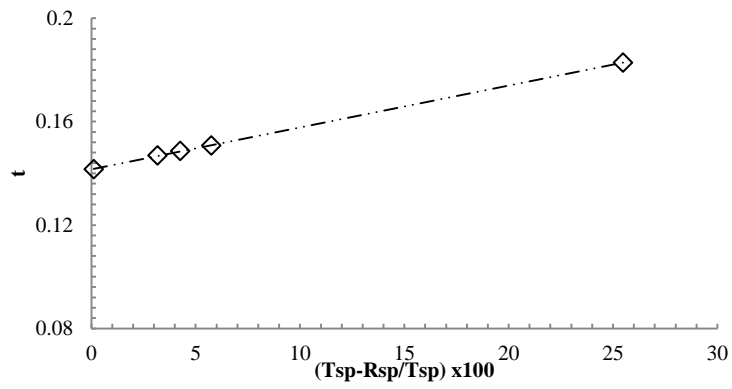


Fig. 10: Error margin in thrust deduction prediction

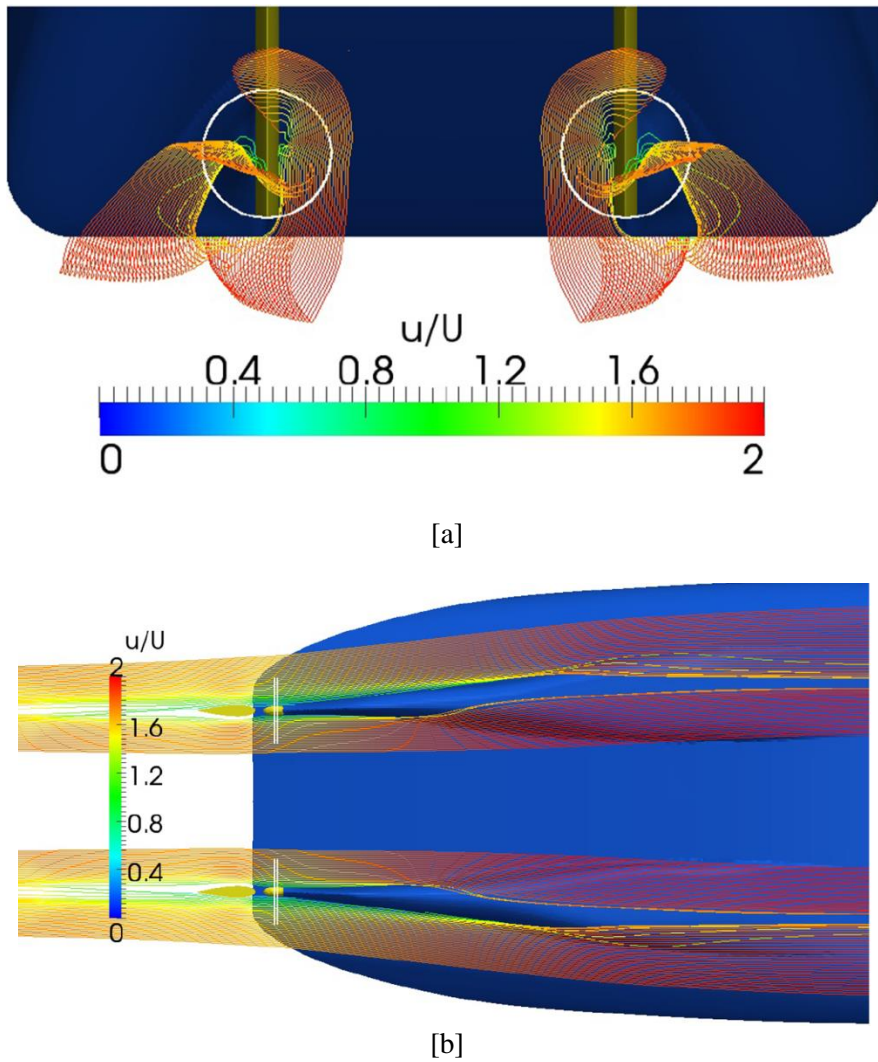


Fig. 11: Streamlines passing through twin skegs at loaded draught, $F_n = 0.197$ [a] view from stern [b] view from bottom.

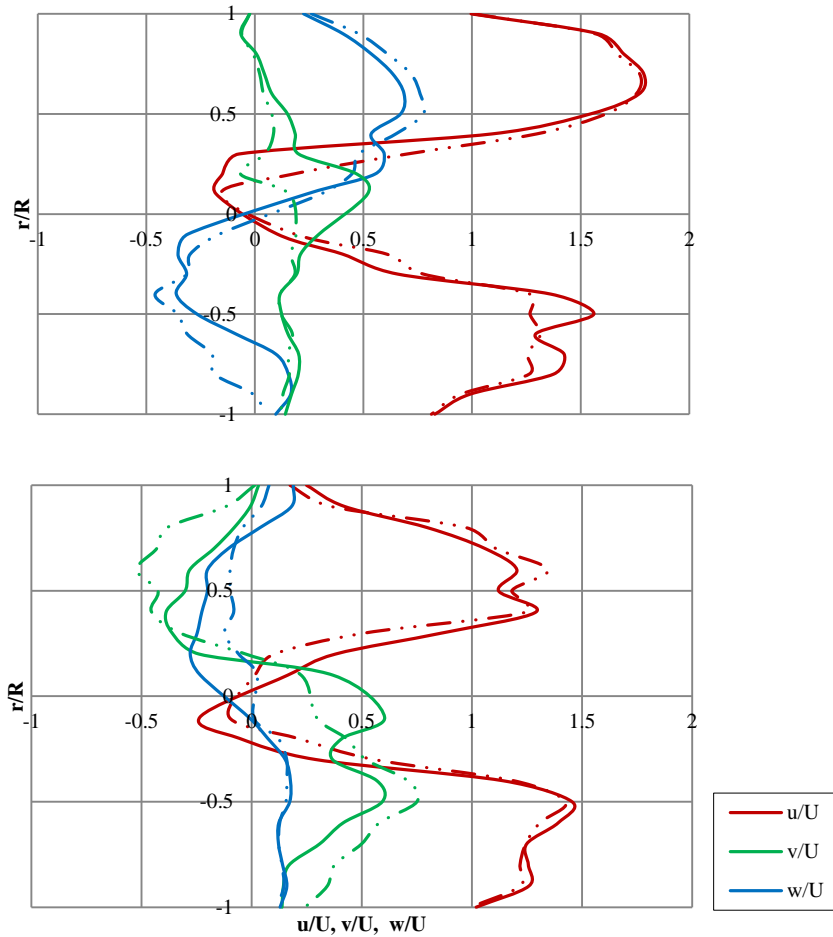


Fig. 12: Wake cut at $0.18D$ behind propeller plane [top] fixed z and varied y [bottom] fixed y and varied z , for loaded draught condition, port side propeller. NB: solid lines represent the addition of tangential wake effect and dotted lines represent no addition of tangential wake effect.

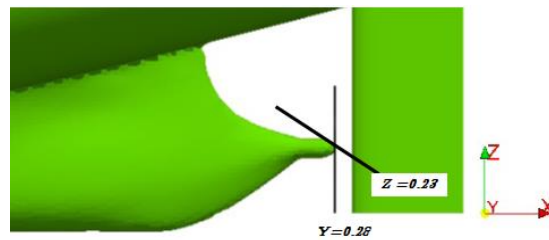


Fig. 13: Wake cut location for plots of velocity at $0.18D$ behind propeller plane

4 Conclusions

In the present paper, the impact of hull-propeller-rudder interaction on ship powering has been presented. Various methodologies which have been used for such successful analysis were discussed along with results into the sensitivity into which the interaction between the propeller and rudder downstream of a skeg is resolved as well as varying the length of the upstream skeg. Overall, good agreement was found between the experimental and computational results when predicting the influence of the skeg and propeller on rudder. However, it can be seen that there is a significant computational expense associated with a time resolved propeller interaction and that alternate body force based methods are likely to still be required for hull(and skeg) -propeller-rudder computations.

References

- BADDOE, C.; WINDEN, B.; LIDTKE, A.K.; PHILLIPS, A.B.; HUDSON, D.A.; TURNOCK, S.R. (2014), *Comparison of various approaches to numerical simulation of ship resistance and propulsion*, SIMMAN 2014, Lyngby
- BADDOE, C.; PHILLIPS, A.B.; TURNOCK, S.R. (2015), *Influence of drift angle on the computation of hull-propeller-rudder interaction*, J.Ocean Eng. 103, pp.64-77
- BADDOE, C. (2015), *Design practice for the stern hull of a future twin-skeg ship using a high fidelity numerical approach*, PhD Thesis, University of Southampton
- DATE, J.C.; TURNOCK, S.R. (2002), *Computational evaluation of the periodic performance of a NACA 0012 fitted with a Gurney flap*. J. Fluids Eng. 124, pp.227-234
- EÇA, L.; HOEKSTRA, M.; WINDT, J. (2002), *Practical Grid Generation Tools with Applications to Ship Hydrodynamics*, 8th Int. Conf. in Grid Generation in Computational Field Simulations, Hawaii
- HOERNER, S. F. (1965), *Fluid dynamic drag*, Midland Park, New Jersey
- HOUGH, G.R.; ORDWAY, D.E. (1965), *The generalized actuator disc*. Dev. in Theor. and Appl. Mech. 2, pp.317-336
- LÜBKE, L. (2005), *Numerical simulation of flow around the propelled KCS*, CFD Workshop Tokyo, Tokyo, pp.587-592
- MOLLAND, A.F.; TURNOCK, S.R.. (2007), *Marine rudders and control surfaces: principles, data, design and applications*, Butterworth-Heinemann, Oxford
- MOLLAND, A.F.; TURNOCK, S.R.; HUDSON, D.A. (2011), *Ship resistance and propulsion: practical estimation of ship propulsive power*, University Press, Cambridge
- PHILLIPS, A.B.; TURNOCK, S.R.; FURLONG, M.E. (2009), *Evaluation of manoeuvring coefficients of a self-propelled ship using a blade element momentum propeller model coupled to a Reynolds averaged Navier Stokes flow solver*, J. Ocean Eng. 36/15, pp.1217-1225
- PHILLIPS, A.B.; TURNOCK, S.R.; FURLONG, M.E. (2010), *Accurate capture of rudder-propeller interaction using a coupled blade element momentum-RANS approach*, Ship Technology Research 57/2, pp.128-139
- SAKAMOTO, N.; KAWANAMI, Y.; UTO, S.; SASAKI, N. (2013), *Estimation of Resistance and Self-propulsion characteristics for a Low L/B Twin-Skeg Container Ship by High-Fidelity RANS Solver*, J. Ship Research, 57/1, pp.24-41
- SIMMAN (2014), *Workshop on verification and validation of ship manoeuvring simulation methods*, Lyngby
- SIMONSEN, C. (2000), *Propeller-Rudder Interaction by RANS*, Ph.D thesis, University of Denmark
- SIMONSEN, C.; STERN, F. (2003), *Verification and Validation of RANS manoeuvring simulation of Esso Osaka: effects of drift and rudder angle on forces and moments*. J. Computers and Fluids 32, pp.1325-1356
- WANG, X.; WALTERS, K. (2012), *Computational analysis of marine propeller performance using transition-sensitive turbulence modelling*, J.Fluids Eng. 134/7, pp.071107